ACS OMEGA

http://pubs.acs.org/journal/acsodf

Article

Inhibitory Capabilities of Sweet Yellow Capsicum Extract toward the Rusting of Steel Rebars in Cement Pore Solution

Mohamed A. Deyab* and Q. Mohsen

Cite This: *ACS Omega* 2023, 8, 3303−3309

Read Online

ACCESS | Metrics & More | Article Recommendations

ABSTRACT: The inhibitory capabilities of the sweet yellow capsicum extract (SYCE) toward the rusting of steel rebars in cement pore solution (CPS) were tested employing the electrochemical and mass loss methods. Gallic acid, caffeic acid, *p*-coumaric acid, ferulic acid, luteolin, and cinnamic acid are the most important constituents in the SYCE extract. By adsorbing them on steel bars, the organic compounds in the CSA extract enable them with an effective mixed-type inhibition, suppressing both anodic and cathodic procedures. At 300 ppm, the highest performances were 95.3 and 97.5% utilizing mass loss and electrochemical approaches, respectively. The activation energy for the corrosion process is greatly increased by the addition of the SYCE extract, going from 13.2 kJ mol^{-1} (blank solution) to 30.0 kJ mol^{-1} (300 ppm SYCE extract). The physical adsorption actions of the SYCE extract are described by the Freundlich equilibrium constant's smallest value, which is 0.074 ppm^{-1}. Many future investigators will be attracted by these discoveries to work relentlessly to uncover the anti-corrosion characteristics of novel plant extracts in the area of concrete additives.

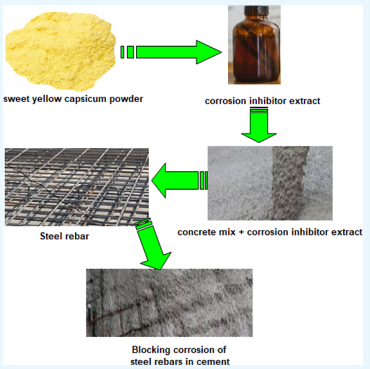

1. INTRODUCTION

Concrete with chloride salts contains corrosion inhibitors, which are used in large buildings, coastal buildings, and bridges.[1−3] Chlorides have the ability to degrade concrete reinforcing steel.[4,5] Inside the alkalinity condition of concrete, ferrous oxide is persistent, but it combines with chloride ions to produce complexes that migrate away from the steel and promote rusting.[6] The chloride ions continue to destroy the steel till the passivating oxide film is eliminated.[7,8] Corrosion inhibitor compounds chemically impede the corrosion operation.[9,10] Inorganic corrosion inhibitors that are commercially accessible include calcium nitrite, sodium nitrite, and phosphates.[11] Such inorganic chemicals are hazardous to the environment and are forbidden in many industries.[12] Another alternative for steel corrosion inhibitors in concrete is to employ organic inhibitors such as alkanolamines and amines, which are commonly used.[13,14] Nevertheless, there are certain concerns concerning the miscibility of organic inhibitors and also their harmful and toxic influences on living beings and concrete. Because of the negative effects of inorganic and organic corrosion inhibitors, the usage of plant extracts as corrosion inhibitors has grown significantly during the last two decades.[15−18]

Harb et al.[19] evaluated the use of the olive leaf extract as an eco corrosion inhibitor for reinforced concrete polluted with saltwater. They discovered that the methanol extract provides the highest inhibition (91.9%). Loto et al.[20] studied the influence of the *Vernonia amygdalina* extract on the corrosion response of implanted mild steel rebar in concrete. At 25% concentration, the smallest inhibitor levels were utilized and the maximum inhibition effectiveness of 90.08% was observed. Asipita et al.[21] employed a *Bambusa arundinacea* extract as a corrosion inhibitor. It already has a pore-blocking ability and inhibits variable oxygenation of concrete, which promotes steel corrosion.

Due to worldwide environmental problems, environmental legislation, and public health issues, numerous scientists in the area of anti-corrosion began to work on environmentally acceptable inhibitors in concrete building processes.[22,23]

We use sweet yellow capsicum extract (SYCE) as an ecologically friendly inhibitor in CPS solutions to increase the corrosion resistance of steel rebars in this article. The primary novelty of this work is to present a new green inhibitor (i.e., SYCE) for steel rebars corrosion in cement pore solution (CPS) and explain its inhibitory effect and processes in order to extend its applicability in the building structural applications. Utilizing electrochemical, mass loss, and surface exploratory tools, the SYCE extract was prepared, characterized, and applied as a corrosion inhibitor for steel rebars in the research work.

Received: October 27, 2022
Accepted: December 26, 2022
Published: January 9, 2023

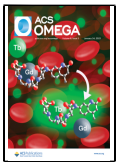

https://doi.org/10.1021/acsomega.2c06639
ACS Omega 2023, 8, 3303−3309

2. EXPERIMENTAL SECTION

2.1. Materials and Solutions. Steel rebar and CPS compositions are presented in Table 1.

Table 1. Steel Rebar and CPS Compositions

steel rebar composition wt %	0.18C, 0.29Mg, 0.020P, 0.003Si, 0.026Al, 0.029Ni, 0.02Cr and the remaining Fe sources: Egypt. Steel company
CPS composition	4 g/L NaOH, 11.2 g/L KOH, 3.5 g/L $Ca(OH)_2$, 0.5 g/L NaCl, 0.43 g/L Na_2SO_4, pH = 13.5sources: EPRI Lab. Preparation

An Egyptian plant company supplied a sweet yellow capsicum powder. At 348 K, 20 g of sweet yellow capsicum powder was refluxed using 100 mL of stocking solutions (60 percent ethanol + 20 percent ethyl acetate + 20 percent distilled H_2O) for 3 h. The refluxed solution was then cleaned using a Buchner funnel. The solution then was condensed in a rotating suction evaporator and left to dry in a pressurized drying furnace at 333 K. The largest and most significant constituents of the SYCE extract were identified by liquid chromatography (shimadzu Instruments) and FTIR (PerkinElmer Instruments).

2.3. Corrosion Rate Measurements. The corrosive rate of reinforcing steel in the CPS liquid was estimated using the mass loss and electrochemical methodology in absence/presence of the SYCE extract. For mass loss studies, ASTM G 31−72 standard practice was applied.[24] The steel samples (dimension = 1.5 cm × 1.0 cm × 0.3 cm) were submerged for 10 days inside a 100 mL CPS solution in the absence/presence of the SYCE extract.

The rate of corrosion (W_{corr}) and the degree protection performance (P_w %) were computed using eqs 1 and 2[25,26]

$$W_{corr} = \frac{W_1 - W_2}{S \times t} \quad (1)$$

$$P_w\ \% = \frac{W^0_{corr} - W_{corr}}{W^0_{corr}} \quad (2)$$

where W_1, W^0_{corr} and W_2,W_{corr} are the mass loss and corrosion rate before and after soaking in CPS solution, respectively. Also, S is the steel surface area and t is experiment time.

A three-electrode crystal unit was utilized for electrochemical testing. This experiment employed a Pt strip (counter element), a saturated calomel electrode (SCE, reference element), and a potentiostat/galvanostat (kinds: Gamry 3000). Potential−current graphs were created in specific circumstances (temperature 298 K, scan rate 0.125 mV s^{-1}, potential field ±250 mV vs OCP).

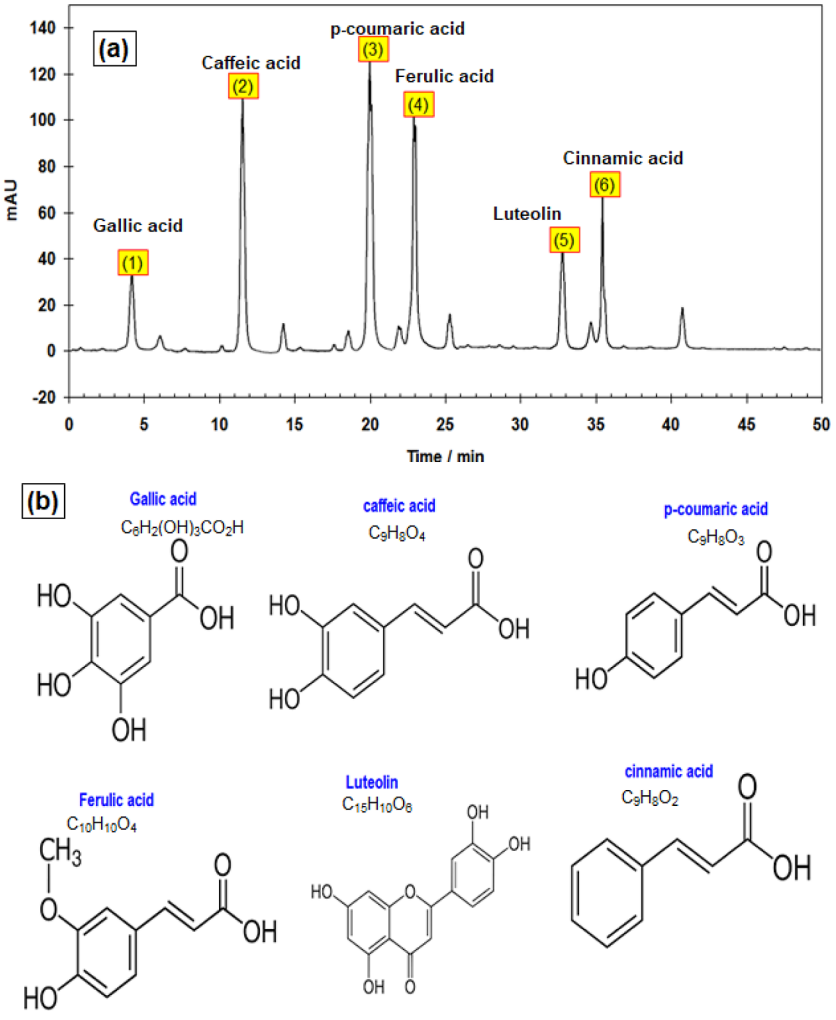

Figure 1. (a) HPLC graph of the SYCE extract and (b) chemical structures of essential parts of the SYCE extract.

https://doi.org/10.1021/acsomega.2c06639
ACS Omega 2023, 8, 3303−3309

The percent protecting performance (P_j %) was computed using the below equation[27]

$$P_j\ \% = \frac{j_{corr(0)} - j_{corr}}{j_{corr(0)}} \times 100 \quad (3)$$

The corrosion current density in the absence/presence of the SYCE extract is represented by $j_{corr(0)}$ and j_{corr}, respectively.

After 24 h of soaking in the solutions, electrochemical impedance spectroscopy (EIS) assays were produced with a 10 mV AC-signal magnitude and a frequency variety of 100 kHz to 10.0 mHz.

The percent protecting performance (E_R %) was computed using the below equation

$$E_R\ \% = \left[1 - \frac{R_{CT0}}{R_{CT}}\right] \times 100 \quad (4)$$

The charge transfer resistance in the absence/presence of the SYCE extract is represented by R_{CT0} and R_{CT0}, respectively.

2.4. Surface Morphology Analyses. Surface morphologies of the steel rebar after submerged for 10 days inside a 100 mL CPS solution in the absence/presence of the 300 ppm SYCE extract were investigated using scanning electron microscopy (SEM) and FTIR (PerkinElmer Instruments).

3. RESULTS AND DISCUSSION

3.1. SYCE Extract Characterization. The essential chemical components of the SYCE extract were investigated using high performance liquid chromatography (HPLC) analysis (see Figure 1a). The active ingredients for the number of bands in the HPLC graph are shown in Figure 1a. The most essential parts of the SYCE extract are gallic acid, caffeic acid, *p*-coumaric acid, ferulic acid, luteolin, and cinnamic acid (see Figure 1b).

Figure 2 shows the FT-IR spectrum of the pure SYCE extract. It contains OH stretching at 3277 cm^{-1}, sym and asym

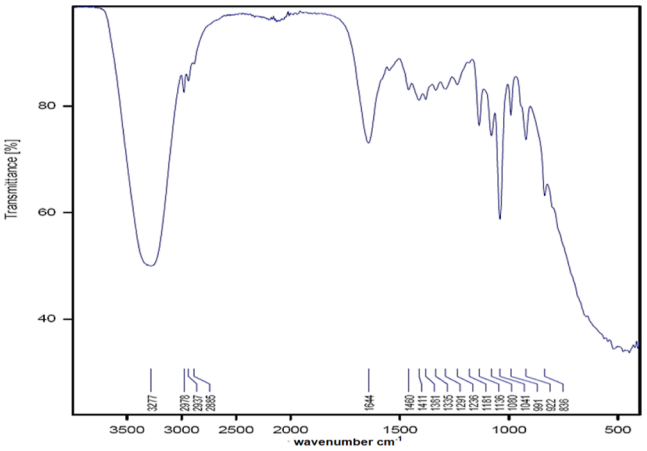

Figure 2. FTIR spectra of the pure SYCE extract.

stretching of CH_3 groups at 2978, 2937, and 2885 cm^{-1}, C═O stretching groups at 1644 cm^{-1}, CH_2 bending at 1460 cm^{-1}, CH_3 bending at 1381 cm^{-1}, C−O stretching at 1291, 1080, and 1041 cm^{-1}, C−O−C stretching at 1236 cm^{-1}, C−H out-of-bending at 991 cm^{-1}, and C−H out-of-plane bending and 922 and 836 cm^{-1}.

3.2. Anti-Corrosion Characteristics of SYCE Extract. The mass loss assay is done to determine the W_{corr} and P_w % of steel rebar pieces dipped in CPS solution including the SYCE extract. Table 2 contains a list of these parameters. Based on

Table 2. Corrosion Rate W_{corr} and Inhibition Efficiency P_w % Values for the Steel Rebar in CPS Solution in the Presence/Absence of the SYCE Extract at 298 K

SYCE extract concn ppm	W_{corr}(μg cm^{-2} h^{-1}) × 10^{-3}	P_w %
blank	16.4 ± 0.42	
50	9.21 ± 0.36	43.8
100	5.57 ± 0.30	66.0
150	1.98 ± 0.17	87.9
200	1.08 ± 0.15	93.4
300	0.77 ± 0.05	95.3

mass loss data, the SYCE extract lowers the corrosion activity of rebar sample dipped in CPS solution. The amount of the SYCE extract has a strong influence on its anti-corrosion efficacy. At the optimal quantity of the SYCE extract (i.e. 300 ppm), the efficiency of the SYCE extract P_w % achieved 95.3%.

The kinetic performance of steel rebar oxidization in CPS medium including the SYCE extract was evaluated using electrochemical experiments. Figure 3 depicts the polarization

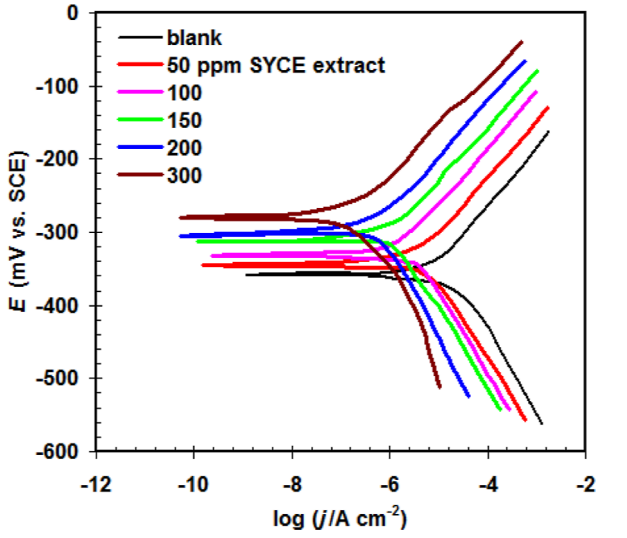

Figure 3. Polarization plot (Tafel form) for the steel rebar in CPS solution in the presence/absence of the SYCE extract at 298 K.

plot (Tafel form). Table 3 provides polarization factors such as corrosion potential (E_{corr}) as well as corrosion current density

Table 3. Polarization Parameters and the Corresponding Corrosion Inhibition Efficiency for the Steel Rebar in CPS Solution in the Presence/Absence of the SYCE Extract at 298 K

SYCE extract concn ppm	j_{corr}(μA cm^{-2})	−E_{corr} mV vs SCE	P_j %
blank	8.56	360	
50	4.46	345	47.8
100	2.52	332	70.5
150	0.83	313	90.3
200	0.44	305	94.8
300	0.23	281	97.3

https://doi.org/10.1021/acsomega.2c06639
ACS Omega 2023, 8, 3303−3309

(j_{corr}). We observed that using the SYCE extract minimizes j_{corr} values to extremely small levels (i.e. 0.23 μA cm^{-2}). For all concentrations, the movements in E_{corr} values as compared to the blank condition generally lower than 85 mV. This demonstrates that the SYCE extract is a mixed category inhibitor.[28,29] The P_j % is shown to grow with increasing SYCE dosage and attain an optimum value (97.3%) at 300 ppm.

Figure 4 shows the EIS plot (Nyquist form) for the steel rebar in CPS solution in the presence/absence of the SYCE extract at 298 K. The size of the semicircle yielded in the CPS solution was the smallest in Figure 4, and the size expanded as the dosage of SYCE extract increased. Table 4 displays the

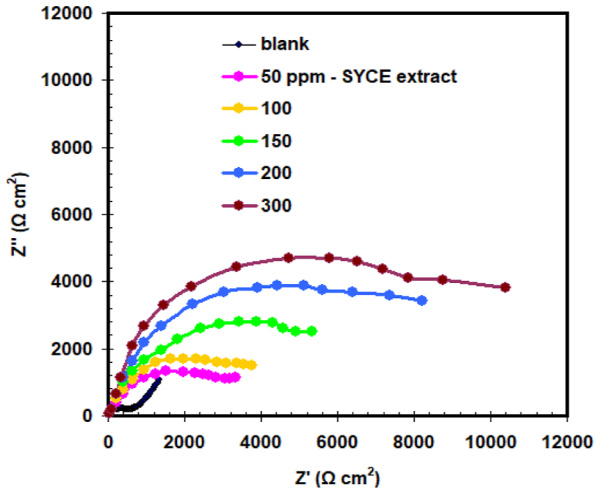

Figure 4. EIS plot (Nyquist form) for the steel rebar in CPS solution in the presence/absence of the SYCE extract at 298 K.

Table 4. EIS Parameters and the Corresponding Corrosion Inhibition Efficiency for the Steel Rebar in CPS Solution in the Presence/Absence of the SYCE Extract at 298 K

SYCE extract concn ppm	R_{ct}Ω cm^2	CPE$_{dl}$(F cm^{-2})	E_R %
blank	678	2.3 × 10^{-5}	
50	1967	1.4 × 10^{-5}	65.5
100	2235	7.1 × 10^{-6}	69.6
150	4898	3.2 × 10^{-6}	86.1
200	6454	2.6 × 10^{-6}	89.4
300	9340	1.7 × 10^{-6}	92.7

quantified values of EIS parameters upon fitting.[30] The R_{ct} is revealed to be maximum for 300 ppm SYCE extract actually contains CPS solution, followed by 200, 150, 100, and 50 ppm, and without SYCE. Solutions containing the SYCE extract have lower CPE$_{dl}$ (constant phase element) values while having higher R_{ct} values. This is because the nearby dielectric constant has decreased while the electrical double layer width has increased. For 300 ppm of the SYCE extract, the received E_R % is 92.7%. The efficiency results from electrochemical analysis and mass loss are consistent between each other.

The SYCE extract's inhibitory mechanism is based on the fundamental ingredients of the extract as well as the physical connection of various functional groups (see Figure 1b). The additional electron donor groups provided, primarily heteroatoms with conjugated double bonds, better inhibitor derivatives' anticorrosion performance.[31] The anti-corrosion abilities of the SYCE extract operate by producing an adsorbed layer on the steel surface.[32] Their effect on the steel surface is based on physical adsorption, which involves the creation of a barrier layer that eliminates water or corrosive ions out from surface.[33] The inhibitory activity of the tested SYCE extract was driven by the connection of aromatic ring electrons and p-electrons of OH groups with unoccupied d-orbitals of steel, via which they created an adherent, solid, and homogeneous thin layer on the steel surface.

3.4. Impacts of Temperature and Thermodynamic Calculation. Temperature is a significant component in the study of corrosion inhibition phenomena.[34] Table 5 depicts the W_{corr} and P_w % of steel rebar in CPS solution with and without the SYCE extract (300 ppm) at several temperatures (298–328 K).

Table 5. Mass Loss Data at Different Temperatures for Steel Rebar in CPS Solution in the Presence/Absence of the SYCE Extract (300 ppm)

temperature (K)	SYCE extract	W_{corr}(μg cm^{-2} h^{-1}) × 10^{-3}	P_w %
298	0	16.4 ± 0.42	
	+	0.77 ± 0.05	95.3
308	0	18.4 ± 0.53	
	+	0.98 ± 0.03	94.6
318	0	22.1 ± 0.43	
	+	1.7 ± 0.22	92.3
328	0	26.6 ± 0.63	
	+	2.2 ± 0.13	91.7

The findings clearly show that the W_{corr} of steel rebar in CPS solution (both control or inhibited) tends to change with temperature. This tendency may be explained by the roughness of the steel rebar surface produced by the higher temperature and also a transform in the adsorption/desorption equilibrium forward into desorption of the SYCE extract from the steel rebar interface.[35]

As the temperature goes up, the P_w % percent decreases consistently (Table 5), reflecting a physisorption activity.[36] Increasing temperatures seemed to have no impact on P_w %, revealing that the SYCE extract/surface interaction is highly stable. The SYCE extract can indeed be considered an acceptable inhibitor, especially at elevated temperatures. The investigation of the Arrhenius (eq 5) and transition state (eq 6) relationships enabled the determination of various variables like activation energy (E_a), enthalpy change (ΔH_a), and entropy change (ΔS_a) to clarify the oxidation activity and the probable method of SYCE extract adsorption.[37,38]

$$\ln W_{corr} = \ln A - \frac{E_a}{RT} \quad (5)$$

$$\ln(W_{corr}/T) = \ln(R/Nh) + (\Delta S_a/R) - (\Delta H_a/RT) \quad (6)$$

(R = molar gas constant, N = 6.2022 1023 mol^{-1}, T = temperature, h = 6.6261 10^{-34} m^2 kg s^{-1}, A = pre-exponential constant).

The Arrhenius profile (Figure 5a) was utilized to assess E_a in the presence and without the SYCE extract (300 ppm). The addition of the SYCE extract greatly enhances the E_a from 13.2 kJ mol^{-1} (blank solution) to 30.0 kJ mol^{-1} (300 ppm SYCE extract). Steel rebar corrosion in CPS solution is retarded by the addition of the SYCE extract, which has high activation energy. The adsorption of the SYCE extract on the surface of steel rebar increases the size of the double layer, raising the

https://doi.org/10.1021/acsomega.2c06639
ACS Omega 2023, 8, 3303−3309

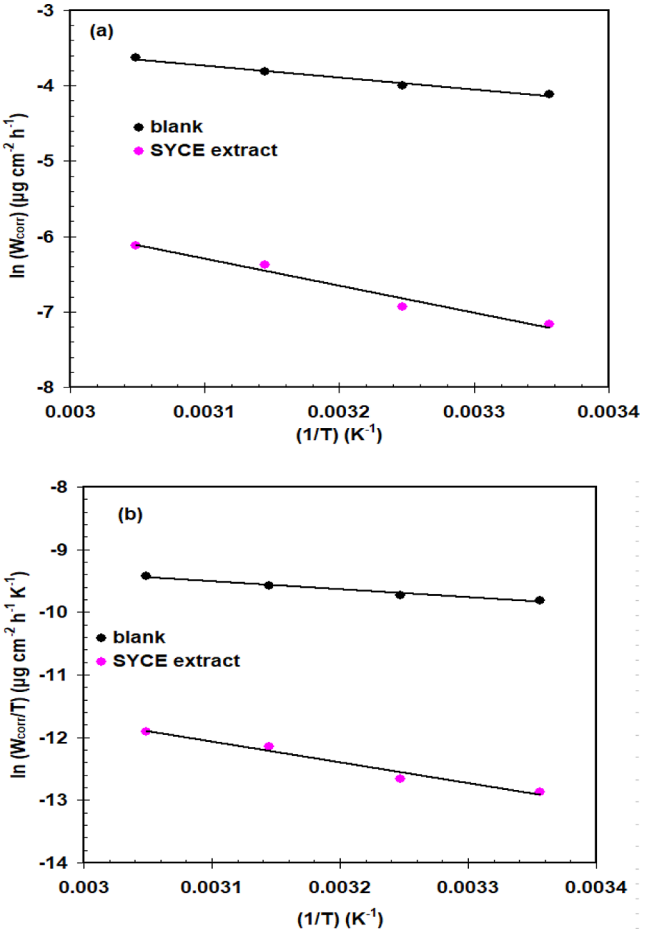

Figure 5. Arrhenius (a) and transition state (b) plots for steel rebar in CPS solution in the presence/absence of the SYCE extract (300 ppm).

energy gap required to activate the corrosion process.[39] This has been attributed to steel rebar molecules' superior physical sorption.[40]

The values of ΔH_a and ΔS_a were calculated using the transition state profile (Figure 5b). The SYCE extract increases the ΔH_a from 10.6 kJ mol^{-1} (blank solution) to 27.4 kJ mol^{-1} (300 ppm SYCE extract). The positive value of ΔH_a[41] signifies that steel rebar oxidation in CPS solution is endothermic. The ΔS_a ranged from −151.4 J mol^{-1} K^{-1} (blank solution) to −182.2 J mol^{-1} K^{-1} (300 ppm SYCE extract). Furthermore, the transition from a negative quantity of ΔS_a in the absence of the SYCE extract toward a more negative quantity of ΔS_a in the addition of SYCE extract might be compared to diminished disorder during the creation of the activated complex in the presence of the SYCE extract.[42]

The Freundlich isotherm concept is an adsorption pattern that assumes a multi-layer adsorption operation with adsorbent desorption occurring on a heterogeneous sorbent. This is an approach that is commonly used to yield an interpretation for the adsorption properties of heterogeneous surfaces.[43] In this study, we used the Freundlich isotherm (eq 7) to explain the adsorption of the SYCE extract on the steel rebar interface.[44]

$$\log(\theta) = \log K_F + \frac{1}{n}\log C_{inh} \quad (7)$$

($\theta = P_w$ %/100, C_{inh} = SYCE extract, $1/n$ = Freundlich slope, K_F = Freundlich equilibrium constant).

The Freundlich isotherm for the SYCE extract is depicted in Figure 6. The linear correlation (R^2) for Figure 6 is

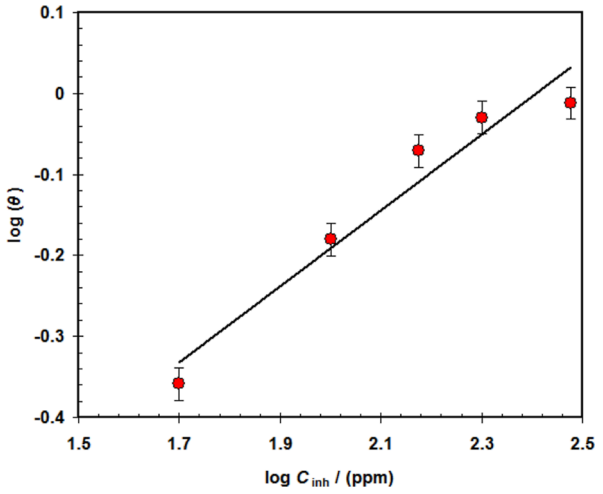

Figure 6. Freundlich isotherm for adsorption of the SYCE extract on steel rebar in CPS solution at 298 K.

significantly nearer to one, confirming that this mode is appropriate for evaluating adsorption tendency.[45] Furthermore, the smallest K_F value (i.e. 0.074 L/mmol) describes the physical adsorption actions of the SYCE extract.[44] The presence of a value of $1/n$ ($1/n$ = 0.468) between 0 and 1 verifies the remarkable adsorption scenarios.[46]

3.3. Examination of the Steel Rebar Surface.

Experimental research SEM examinations were supplemented with quantified FT-IR analysis to validate the findings from the electrochemical and mass loss experiments.

In Figure 7a, a SEM surface view of the steel rebar in CPS solution without the SYCE extract reveals that the irregular

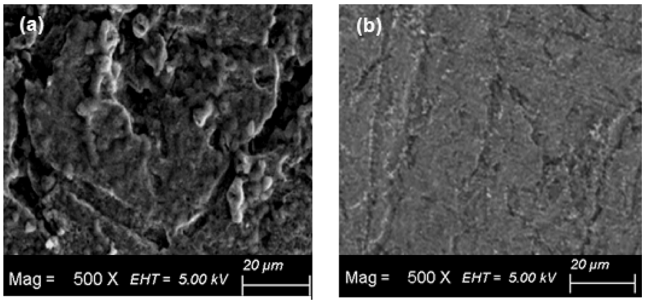

Figure 7. SEM images for steel rebar surface: (a) exposed to blank CPS solution and (b) exposed to CPS solution containing the 300 ppm SYCE extract.

rusting over a steel surface is highly thick and visible. As shown in the SEM image (Figure 7b), adding 300 ppm of the SYCE extract to CPS solution lowers the level of corrosion on the steel surface.

The FT-IR spectra of the SYCE extract and the layer produced on steel rebar in CPS solution containing the SYCE extract are shown in Figures 2 and 8, respectively. The characteristic absorption bands of the SYCE extract can indeed be seen in FTIR spectra of Figure 8. It contains OH stretching (3212 cm^{-1}), sym and asym stretching of CH_3 groups (2972 and 2923 cm^{-1}), C═O stretching groups (1637 cm^{-1}), CH_2 bending (1454 cm^{-1}), CH_3 bending (1376 cm^{-1}), C−O

https://doi.org/10.1021/acsomega.2c06639
ACS Omega 2023, 8, 3303−3309

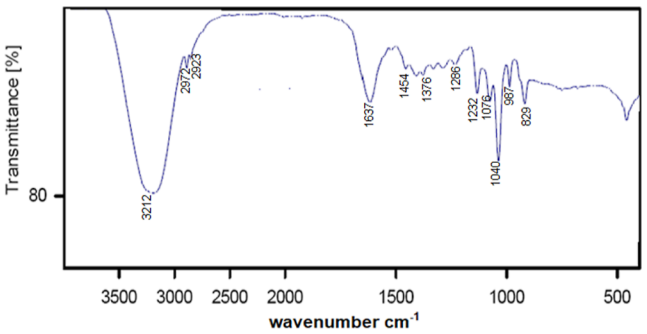

Figure 8. FT-IR spectra of layer produced on steel rebar in CPS solution containing the SYCE extract.

stretching (1286, 1076 and 1040 cm^{-1}), C−O−C stretching (1232 cm^{-1}), C−H out-of-bending (987 cm^{-1}), and C−H out-of-plane bending (829 cm^{-1}). This spectrum displays that O and π-electrons (aromatic ring) may form covalent connections with the surface of steel rebar. When comparing FTIR spectra in Figure 8 to spectra in Figure 2, the position of the O−H and C−H peaks has shifted together low intensity, indicating that these groups interact in the adsorption process.[46]

4. CONCLUSIONS

In order to broaden its applicability in the building structural applications, this research introduces a new green inhibitor (i.e. SYCE) for steel rebar corrosion in CPS and explains its inhibitory effect and processes.The most important constituents of the SYCE extract are gallic acid, caffeic acid, *p*-coumaric acid, ferulic acid, luteolin, and cinnamic acid. At concentrations of 300 ppm, SYCE demonstrated the highest inhibition efficacies, with values of 95.3 and 97.5%, respectively, for mass loss and electrochemical methods. The SYCE extract functions as a combined corrosion inhibitor, slowing both anodic and cathodic reactions, according to Tafel curves. The presence of the SYCE extract significantly increases the activation energy for the electrochemical reactions, increasing it from 13.2 kJ mol^{-1} (blank solution) to 30.0 kJ mol^{-1} (300 ppm SYCE extract). The smallest value of the Freundlich equilibrium constant, 0.074 ppm^{-1}, describes the physical adsorption actions of the SYCE extract. SEM and FT-IR surface inspection results support the adsorption of SYCE extract ingredients on steel surfaces. The current findings cleared the path for future efforts to increase corrosion protection efficiency through the use of non-toxic compounds.

■ ASSOCIATED CONTENT

Data Availability Statement

The data sets used and/or analyzed during the current study are available from the corresponding author on reasonable request.

■ AUTHOR INFORMATION

Corresponding Author

Mohamed A. Deyab − *Egyptian Petroleum Research Institute (EPRI), Cairo 11727, Egypt;* orcid.org/0000-0002-4053-4942; Phone: +201006137150; Email: hamadadeiab@yahoo.com; Fax: +202 22747433

Author

Q. Mohsen − *Department of Chemistry, College of Sciences, Taif University, Taif 11099, Saudi Arabia*

Complete contact information is available at: https://pubs.acs.org/10.1021/acsomega.2c06639

Notes

The authors declare no competing financial interest.

■ ACKNOWLEDGMENTS

This work was supported by Taif University Researchers Supporting Project number (TURSP-2020/19), Taif University, Saudi Arabia. The authors gratefully acknowledge the support of the "Egyptian Academy of Scientific Research and Technology". Also, we are grateful for the help of the Egyptian Petroleum Research Institute.

■ REFERENCES

(1) Das, J. K.; Pradhan, B. Study on influence of nitrite and phosphate based inhibiting admixtures on chloride interaction, rebar corrosion. and microstructure of concrete subjected to different chloride exposures. *J. Build. Eng.* **2022**, *50*, 104192.

(2) Lapiro, I.; Mezhov, A.; Kovler, K. Performance of corrosion inhibitors in reinforced concrete elements under electrical voltage. *Constr. Build. Mater.* **2022**, *342*, 127656.

(3) Zhang, L.; Pan, Y.; Xu, K.; Bi, L.; Chen, M.; Han, B. Corrosion behavior of concrete fabricated with lithium slag as corrosion inhibitor under simulated acid rain corrosion action. *J. Cleaner Prod.* **2022**, *377*, 134300.

(4) Liu, Y.; Shi, J. Corrosion resistance of carbon steel in alkaline concrete pore solutions containing phytate and chloride ions. *Corros. Sci.* **2022**, *205*, 110451.

(5) Foad El-Sherbini, E. E.; Abd-El-Wahab, S. M.; Amin, M. A.; Deyab, M. A. Electrochemical behavior of tin in sodium borate solutions and the effect of halide ions and some inorganic inhibitors. *Corros. Sci.* **2006**, *48*, 1885−1898.

(6) Broomfield, J. P.*Corrosion of Steel in Concrete: Understanding, Investigation and Repair*; Taylor & Francis: London and New York, 2006; Vol. 2.

(7) Bertolini, L.; Elsener, B.; Pedeferri, P.; Polder, R. B.*Corrosion of Steel in Concrete: Prevention, Diagnosis, Repair*; Wiley-VCH Verlag GmbH & Co. KgaA: Weinheim, 2004.

(8) Deyab, M. A.; Keera, S. T. Cyclic voltammetric studies of carbon steel corrosion in chloride -formation water solution and effect of some inorganic salts. *Egypt. J. Pet.* **2012**, *21*, 31−36.

(9) Mandal, S.; Singh, J. K.; Mallapur, S.; Lee, D.-E.; Park, T. Effect of triethanolamine and sodium hexametaphosphate on formation, growth and breakdown of passive layer in concrete pore solution. *J. Build. Eng.* **2022**, *59*, 105113.

(10) Yuvaraj, S.; Nirmalkumar, K.; Rajesh Kumar, V.; Gayathri, R.; Mukilan, K.; Shubikksha, S. Influence of corrosion inhibitors in reinforced concrete−A state of art of review. *Mater. Today: Proc.* **2022**, *68*, 2406−2412.

(11) Al-Sodani, K. A. A.; Al-Amoudi, O. S. B.; Maslehuddin, M.; Shameem, M. Efficiency of corrosion inhibitors in mitigating corrosion of steel under elevated temperature and chloride concentration. *Constr. Build. Mater.* **2018**, *163*, 97−112.

(12) Wasewar, K. L.; Singh, S.; Kansal, S. K.Chapter 13-Process intensification of treatment of inorganic water pollutants. In *Inorganic Pollutants in Water*; Devi, P., Singh, P., Kansal, S. K., Eds.; Elsevier, 2020; pp 245−271.

(13) Martinez, S.; Valek, L.; Oslaković, I. Adsorption of Organic Anions on Low-Carbon Steel in Saturated Ca $(OH)_2$ and the HSAB Principle. *J. Electrochem. Soc.* **2007**, *154*, C671−C677.

(14) Bolzoni, F.; Brenna, A.; Brenna, G.; Fumagalli, S.; Goidanich, L.; Lazzari, M.; Ormellese, M. P.; Pedeferri, M. Experiences on

https://doi.org/10.1021/acsomega.2c06639
ACS Omega 2023, 8, 3303−3309

corrosion inhibitors for reinforced concrete. *Int. J. Corros. Scale Inhib.* **2014**, *3*, 254−278.
(15) Raja, P. B.; Sethuraman, M. G. Natural products as corrosion inhibitor for metals in corrosive media - A review. *Mater. Lett.* **2008**, *62*, 113−116.
(16) Michael, N. C. The Corrosion Inhibition of Mild Steel in Sulphuric Acid Solution by Flavonoid (Catechin) Separated from Nypa Fruticans Wurmb Leaves Extract. *Sci. J. Chem.* **2014**, *2*, 27−32.
(17) Souza, F. S.; Spinelli, A. Caffeic acid as a green corrosion inhibitor for mild steel. *Corros. Sci.* **2009**, *51*, 642−649.
(18) Ikeuba, I.; Ita, B. I.; Okafor, P. C.; Ugi, B. U.; Kporokpo, E. B. Green corrosion inhibitors for mild steel in H_2SO_4 solution: Comparative study of flavonoids extracted from gongronema latifoliunm with crude the extract. *Prot. Met. Phys. Chem. Surf.* **2015**, *51*, 1043−1049.
(19) Harb, M. B.; Abubshait, S.; Etteyeb, N.; Kamoun, M.; Dhouib, A. Olive leaf extract as a green corrosion inhibitor of reinforced concrete contaminated with seawater. *Arabian J. Chem.* **2020**, *13*, 4846−4856.
(20) Loto, C. A.; Joseph, O. O.; Loto, R. T.; Popoola, A. P. I. Inhibition effect of vernoniaamygdalinaextract on the corrosion of mild steel reinforcement in concrete in 3.5M NaCl environment. *Int. J. Electrochem. Sci.* **2013**, *8*, 11087−11100.
(21) Asipita, S. A.; Ismail, M.; Majid, M. Z.; Majid, Z. A.; Abdullah, C.; Mirza, J. Green BambusaArundinacea leaves extract as a sustainable corrosion inhibitor in steel reinforced concrete. *J. Cleaner Prod.* **2014**, *67*, 139−146.
(22) Chauhan, D. S.; Quraishi, M. A.; Qurashi, A. Recent trends in environmentally sustainable Sweet corrosion inhibitors. *J. Mol. Liq.* **2021**, *326*, 115117.
(23) Verma, C.; Haque, J.; Quraishi, M. A.; Ebenso, E. E. Aqueous phase environmental friendly organic corrosion inhibitors derived from one step multicomponent reactions: A review. *J. Mol. Liq.* **2019**, *275*, 18−40.
(24) *ASTM G31-72(2004), Standard Practice for Laboratory Immersion Corrosion Testing of Metals*; ASTM International: West Conshohocken, PA, 2004; www.astm.org.
(25) Nessim, M. I.; Zaky, M. T.; Deyab, M. A. Three new gemini ionic liquids: Synthesis, characterizations and anticorrosion applications. *J. Mol. Liq.* **2018**, *266*, 703−710.
(26) Pal, A.; Das, C. A novel use of solid waste extract from tea factory as corrosion inhibitor in acidic media on boiler quality steel. *Ind. Crops Prod.* **2020**, *151*, 112468.
(27) Deyab, M. A.; Mele, G. Stainless steel bipolar plate coated with polyaniline/Zn-Porphyrin composites coatings for proton exchange membrane fuel cell. *Sci. Rep.* **2020**, *10*, 3277.
(28) Verma, C.; Olasunkanmi, L. O.; Ebenso, E. E.; Quraishi, M. A. Adsorption characteristics of green 5-arylaminomethylene pyrimidine-2,4,6-triones on mild steel surface in acidic medium: experimental and computational approach. *Results Phys.* **2018**, *8*, 657−670.
(29) Zaky, M. T.; Nessim, M. I.; Deyab, M. A. Synthesis of new ionic liquids based on dicationic imidazolium and their anti-corrosion performances. *J. Mol. Liq.* **2019**, *290*, 111230.
(30) Deyab, M. A.; Hamdi, N.; Lachkar, M.; Bali, B. Clay/Phosphate/Epoxy nanocomposites for enhanced coating activity towards corrosion resistance. *Prog. Org. Coat.* **2018**, *123*, 232−237.
(31) Abd El-Rehim, S. S.; Hassan, H. H.; Deyab, M. A.; Abd El Moneim, A. Experimental and theoretical investigations of adsorption and inhibitive properties of Tween 80 on corrosion of aluminum alloy (A5754) in alkaline media. *Z. Phys. Chem.* **2016**, *230*, 67−78.
(32) Deyab, M. A.; El-Rehim, S. S.; Keera, S. T. Study of the effect of association between anionic surfactant and neutral copolymer on the corrosion behaviour of carbon steel in cyclohexane propionic acid. *Colloids Surf., A* **2009**, *348*, 170−176.
(33) Shahmoradi, A. R.; Ranjbarghanei, M.; Javidparvar, A. A.; Guo, L.; Berdimurodov, E.; Ramezanzadeh, B. Theoretical and surface/electrochemical investigations of walnut fruit green husk extract as effective inhibitor for mild-steel corrosion in 1M HCl electrolyte. *J. Mol. Liq.* **2021**, *338*, 116550.
(34) El-Taib Heakal, F.; Deyab, M. A.; Osman, M. M.; Nessim, M. I.; Elkholy, A. E. Synthesis and assessment of new cationic Gemini surfactants as inhibitors for carbon steel corrosion in oilfield water. *RSC Adv.* **2017**, *7*, 47335−47352.
(35) Arrousse, N.; Salim, R.; Abdellaoui, A.; Hajjaji, F.; Hammouti, B.; Mabrouk, E.; Diño, W.; Taleb, M. Synthesis, characterization, and evaluation of xanthene derivative as highly effective, nontoxic corrosion inhibitor for mild steel immersed in 1 M HCl solution. *J. Taiwan Inst. Chem. Eng.* **2021**, *120*, 344−359.
(36) Deyab, M. A.; Fouda, A. S.; Osman, M. M.; Abdel-Fattah, S. Mitigation of acid corrosion on carbon steel by novel pyrazolone derivatives. *RSC Adv.* **2017**, *7*, 45232−45240.
(37) Mobin, M.; Aslam, R.; Aslam, J. Non toxic biodegradable cationic gemini surfactants as novel corrosion inhibitor for mild steel in hydrochloric acid medium and synergistic effect of sodium salicylate: experimental and theoretical approach. *Mater. Chem. Phys.* **2017**, *191*, 151−167.
(38) Deyab, M. A. Understanding the anti-corrosion mechanism and performance of ionic liquids in desalination, petroleum, pickling, descaling, and acid cleaning applications. *J. Mol. Liq.* **2020**, *309*, 113107.
(39) Elayyachy, M.; Elkodadi, M.; Aouniti, A.; Ramdani, A.; Hammouti, B.; Malek, F.; Elidrissi, A. New bipyrazole derivatives as corrosion inhibitors for steel in hydrochloric acid solutions. *J. Mater. Chem. Phys.* **2005**, *93*, 281−285.
(40) Ouakki, M.; Galai, M.; Rbaa, M.; Abousalem, A. S.; Lakhrissi, B.; Touhami, M.; Cherkaoui, M. Electrochemical, thermodynamic and theoretical studies of some imidazole derivatives compounds as acid corrosion inhibitors for mild steel. *J. Mol. Liq.* **2020**, *319*, 114063.
(41) Ansari, K. R.; Quraishi, M. A.; Singh, A. Schiff's base of pyridyl substituted triazoles as new and effective corrosion inhibitors for mild steel in hydrochloric acid solution. *Corros. Sci.* **2014**, *79*, 5−15.
(42) Ech-chihbi, E.; Nahlé, A.; Salim, R.; Benhiba, F.; Moussaif, A.; El-Hajjaji, F.; Oudda, H.; Guenbour, A.; Taleb, M.; Warad, I.; Zarrouk, A. Computational, MD simulation, SEM/EDX and experimental studies for understanding adsorption of benzimidazole derivatives as corrosion inhibitors in 1.0 M HCl solution. *J. Alloys Compd.* **2020**, *844*, 155842.
(43) Ge, D.; Shi, W.; Ren, L.; Zhang, F.; Zhang, G.; Zhang, X.; Zhang, Q. Variation analysis of affinity-membrane model based on Freundlich adsorption. *J. Chromatogr. A* **2006**, *1114*, 40−44.
(44) Deyab, M. A. M. Corrosion inhibition and adsorption behavior of sodium lauryl ether sulfate on l80 carbon steel in acetic acid solution and its synergism with ethanol. *J. Surfactants Deterg.* **2015**, *18*, 405−411.
(45) Deyab, M. A. Hydrogen evolution inhibition by L-serine at the negative electrode of a lead−acid battery. *RSC Adv.* **2015**, *5*, 41365−41371.
(46) Nnaji, N.; Nwaji, N.; Mack, J.; Nyokong, T. Corrosion Resistance of Aluminum against Acid Activation: Impact of Benzothiazole-Substituted Gallium Phthalocyanine. *Molecules* **2019**, *24*, 207.

https://doi.org/10.1021/acsomega.2c06639
ACS Omega 2023, 8, 3303−3309